Int. J. Heat Mass Transfer. Vol. 34, No. 4/5, pp. 1227–1236, 1991
Printed in Great Britain

0017-9310/91 $3.00+0.00

The effect of inclination on local heat transfer under an axisymmetric, free liquid jet

J. STEVENS and B. W. WEBB
Heat Transfer Laboratory, Brigham Young University, Provo, UT 84602, U.S.A.

(*Received* 5 *March* 1990 *and in final form* 15 *June* 1990)

Abstract—The effect of jet inclination on the local heat transfer under an obliquely impinging, round, free liquid jet striking a constant heat flux surface is investigated experimentally. The problem parameters investigated are jet Reynolds number in the range 6600–52 000, and jet inclination, ranging from 40 to 90 deg, measured from the horizontal. Experiments are carried out for nozzle sizes, $d = 4.6$ and 9.3 mm. It is found that the point of maximum heat transfer along the x-axis (the line of intersection of the jet inclination plane with the impingement surface) is shifted upstream (with respect to the jet flow) as a function of jet inclination with a maximum observed shift of 0.5 nozzle diameters. In addition, it is found that the shape of local Nusselt number profiles along the x-axis changed as the jet is inclined. One of these changes is a sharpening of the peak in the profile at the point of maximum heat transfer. Another change is an increasing asymmetry around the point of maximum heat transfer with the upstream side of the profile dropping off more rapidly than the downstream side. Some measurements are taken to characterize the full two-dimensional heat transfer distribution under the inclined jet. Correlations are developed for the radial variation of local heat transfer in the plane of nozzle inclination.

INTRODUCTION

IMPINGING jets are characterized by unusually high transfer coefficients and, consequently, have been widely used for cooling and drying in a variety of industries. Substantial research exists characterizing the transfer coefficients under various configurations of impinging jets.

Impinging jets can be grouped according to several broad characteristics. In general, an impinging jet is termed a submerged jet if it is a gas jet issuing into a gas, or a liquid jet issuing into a liquid, and will be termed a free jet if it is a liquid jet issuing into a gas. In addition, impinging jets can be classified by their shape, their temperature relative to the surface against which they are impinging, whether the jet is oriented normally or obliquely with respect to the impingement surface, and whether the impingement surface is flat or curved.

The purpose of this investigation was to examine the effect of jet inclination on the heat transfer under a round, single-phase free liquid jet impinging on a flat, constant heat-flux surface.

A significant amount of literature exists on transfer coefficients under impinging jets. Reviews of previous work on jet impingement can be found in refs. [1–3]. Martin [4], and Downs and James [5], also reviewed recent work on jet impingement.

Oblique jet impingement has been treated by several investigators. Beltaos [6] examined experimentally and analytically the pressure and shear stress distributions under obliquely impinging axisymmetric air jets. Foss [7], and Foss and Kleis [8] also studied the flow field under an impinging air jet, the former reference treating the case of large impingement angle, the latter treating the small impingement angle case. Donaldson and Snedeker [9] included pressure distribution measurements under an oblique axisymmetric air jet as part of a larger study of jet impingement. They found that for a normalized nozzle-to-plate spacing of $z/d = 1.96$, the x-axis location of the point of maximum pressure is strongly dependent on inclination angle. Rubel [10] carried out numerical calculations in order to characterize the flow field for an axisymmetric air jet at large impingement angles.

Submerged slot jets were studied by Dorrepaal [11] who provided a similarity solution to the Navier–Stokes equation for an inclined jet, and Garg and Jayaraj [12] who studied numerically the flow and heat transfer for a laminar oblique slot jet. In addition, McMurray *et al.* [13] investigated experimentally local heat transfer under an inclined liquid slot jet. Rubel [14] examined the azimuthal redistribution of impingement momentum under an inclined axisymmetric liquid jet.

Goldstein and Franchett [15] studied the effect of jet inclination on the heat transfer under an axisymmetric air jet using a liquid crystal measurement technique for the Reynolds number range $10\,000 \leqslant Re \leqslant 35\,000$. They found that the magnitude of the dimensionless displacement of the point of maximum heat transfer, $|s/d|$, increased monotonically from 0 to 1.5 for $z/d = 4$ and from 0 to 1.9 for $z/d = 10$ as α (jet angle with respect to the horizontal) was decreased from 90 to 30 deg. They also found that near peak Nusselt number, dropped 5–30% with decreasing α, and that this effect was more pronounced with increasing z/d (dimensionless nozzle-to-plate spacing). In addition, the x-axis Nusselt number profiles showed that the heat transfer dropped more steeply on the upstream side than on the downstream side.

Sparrow and Lovell [16] used local mass transfer techniques to evaluate the effect of jet inclination on

NOMENCLATURE

d	jet diameter
h	local heat transfer coefficient, $q_w/(T_s - T_j)$
k	thermal conductivity
Nu	local Nusselt number based on jet diameter, hd/k
Nu_{max}	maximum Nusselt number
Pr	fluid Prandtl number evaluated at the jet exit temperature
q_w	wall heat flux imposed at the heating plate
Q	volumetric flow rate
r	radial distance from the jet centerline–impingement plane intersection, Fig. 1
s	radial location of point of maximum heat transfer after jet inclination, Fig. 1
Re	Reynolds number based on jet diameter, $4Q/\pi\nu d$
T_s	local surface temperature of the isoflux heated plate
T_j	jet exit temperature
U	infinite jet freestream velocity
x	coordinate along the line of intersection of the jet inclination plane with the impingement surface for $\phi = 0$ deg, Fig. 1
z	nozzle-to-plate spacing, Fig. 1.

Greek symbols

α	polar angle of jet inclination measured from the horizontal, Fig. 1
ν	kinematic viscosity
ϕ	azimuthal angle of the plane of jet inclination measured from the negative x-axis, Fig. 1.

an axisymmetric air jet for $Re < 10\,000$. The point of maximum heat transfer was seen to shift 0.4–1.4 diameters for $z/d = 10$, and 0.28–1.1 for $z/d = 7$ as α varied between 90 and 30 deg. The shift in position of the peak heat transfer was accompanied by decreases of 15–20% in the magnitude of the maximum transfer coefficient with increasing inclination. The local transfer coefficient along the x-axis was found to drop more rapidly on the upstream side than on the downstream side and this effect was accentuated at higher nozzle inclinations. It was observed that in an asymmetric flow such as that under an obliquely impinging jet, the point of maximum heat transfer may not coincide with the stagnation point.

Examination of the relevant literature reveals no prior research describing the local heat transfer under an obliquely impinging, axisymmetric free liquid jet. The purpose of this study was to characterize the effect of impingement angle on the two-dimensional heat transfer field beneath such a jet.

APPARATUS AND EXPERIMENTAL METHOD

Figure 1 illustrates the nomenclature used in this study. The radial coordinate, r, is measured from the geometric intersection of the nozzle axis with the impingement plane. The nozzle is inclined from the normal impingement position an angle α measured from the horizontal, and may be rotated an azimuthal angle ϕ. The x-axis is the line of intersection of the jet inclination plane with the impingement plane for $\phi = 0$ deg. Thus, away from the impingement region, $r > 0$ corresponds to 'downstream' with respect to the mean jet flow.

Figure 2 presents a schematic of the nozzle adjustment apparatus and the heated plate. Water was supplied to the nozzle from a laboratory outlet. Before reaching the nozzle, the water passed through two flowmeters which provided a combined measurement range of 0.0063 to 0.76 l s^{-1} (0.1–12 gpm) with an accuracy of 0.0006 l s^{-1}. A thermocouple in the pipe immediately downstream from the flowmeters was used to measure the water temperature, which was very nearly 10°C for all tests. The corresponding fluid Prandtl number at the jet exit is 9.4. Nozzles consisted of glass tubes of 4.6 and 9.3 mm i.d. The outlet end of each tube was carefully ground smooth, flat, and perpendicular to the jet axis. Tube lengths were chosen to be over 50 diameters in order to insure fully developed (turbulent) flow at the nozzle exit. The nozzle adjustment apparatus was designed to allow polar (α) and azimuthal (ϕ) nozzle angle positioning while maintaining the geometric intersection of the jet axis with the impingement plane at a fixed point, and also maintaining a constant distance between that

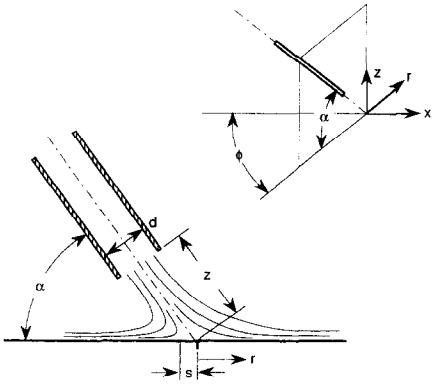

FIG. 1. Schematic of inclined jet and definition of problem geometric parameters.

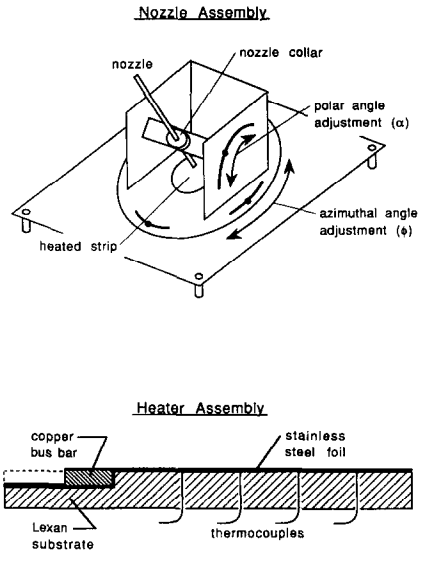

FIG. 2. Schematic of inclined jet and heater assemblies.

point and the nozzle exit. The polar angle (α) adjustment consisted of a nozzle collar support bracket which could move in circular tracks milled in vertical parallel plates (Fig. 2). The circular tracks were cut at a constant radius from the precise point of intersection of the jet axis with the impingement surface using a numerically-controlled mill. Angle markings were scribed on the surfaces of the vertical plates with an estimated angular uncertainty of ± 1 deg. Azimuthal positioning (ϕ) was accomplished by allowing the entire nozzle collar/polar angle positioning apparatus to rotate about a vertical axis in circular tracks milled into the horizontal base plate. Registration of the azimuthal angle position was also achieved with scribed markings on the base plate, again with an estimated uncertainty of ± 1 deg. While the collar securing the nozzle permitted variation of the nozzle-to-plate spacing, that capability was not used in this research and all measurements were made with the nozzle exit at a distance of 15 mm from the impingement point. This corresponds to dimensionless nozzle-to-plate spacings of $z/d = 3.2$ and 1.6 for the 4.6 and 9.3 mm diameter nozzles, respectively. A single nozzle-to-plate spacing was studied for each nozzle diameter since a previous investigation showed only a slight dependence of the local heat transfer on z/d [17].

A schematic cross section of the instrumented heating plate is also illustrated in Fig. 2. The heating element consisted of a rectangular piece of 0.051 mm thick stainless steel (type 302) shim stock. The shim stock was 1.5 cm wide, with approximately 8.0 cm of heated length. It was secured to a backing of 12.7 mm thick Lexan using Dow Corning Silicone rubber sealant. The silicone rubber was used in order to provide adhesion despite the thermal expansion of the heating foil. The metallic foil was mounted directly on the Lexan substrate, and the slight step between the foil edge and the substrate was filled with sealant to form a smooth impingement flow surface. The Lexan backing was prepared by using a numerically controlled mill to cut two depressions in the Lexan to allow for placement of the bus bars and power leads at each end of the heater strip.

Twenty-eight holes, 1.5 mm in diameter on 2.5 mm centers were drilled in the Lexan substrate for thermocouple placement. The mill was used in order to allow precise positioning of the thermocouple holes. After the shim stock was cemented in place, thermocouples (fabricated from 0.127 mm diameter Cu–Co wire) were passed through the holes in the Lexan sheet and were attached directly to the underside of the shim stock with Loctite QM-50 epoxy. This provided intimate thermal contact between the thermocouples and the heating plate. Good contact was insured by checking for electrical continuity between the heater foil and the thermocouples. Although the thermocouple beads were much smaller, the 1.5 mm diameter holes were required so that the bared thermocouple leads would not be crushed together in the holes causing an erroneous reading. This did, however, contribute to uncertainty in the measurement position. Possible electrical interaction between the thermocouple beads and the current in the foil was assessed during an earlier test by reversing the polarity of the power leads while the heated plate was subjected to a typical flow and heating situation (the foil carrying approximately 50 A). Reversing the voltage gradient in the foil in this way resulted in less than 3% change in the local Nusselt number near the stagnation point, with approximately 5% change elsewhere. Reversing the polarity of the d.c. power in the metallic foil would result in a consistent and significant offset in the measured voltages (temperatures) if the thermocouples were affected by the current in the foil. However, no such offset was observed, and the small variation in Nu, which is less than the uncertainty in the Nusselt number, may be attributed to slightly different conduction losses in the bus bars due to transient heatup of the apparatus during the different experiments conducted for each polarity configuration. In spite of the expected high heat transfer coefficients, the shim stock was characterized by a low Biot number (typically 0.017–0.1) making it reasonable to assume that the temperature of the back surface of the shim stock was identical to that of the surface exposed to the fluid.

Copper bus bars, 1.5 cm wide, 2.0 cm long and approximately 2 mm thick were soldered directly to the shim stock. Power leads were soldered to the bus bar on the opposite side from the foil and connected to an HP model 6011 A d.c. power supply (0–20 V, 0–120 A, 1000 W). Voltage measurements were made with voltage taps and a digital multimeter at marked locations on the foil. The voltage probe locations were 67.5 mm apart. Electrical current measurements were made from the power supply readout. Voltage and current measurements were estimated to be accurate to within 0.01 V and 0.1 A, respectively. The heat flux

from the plate was calculated as the product of the voltage and current readings divided by the surface area of the foil between the voltage probe locations. All thermocouples were read to 1.0 μV from an HP model 3497 A data acquisition system with software cold junction compensation. The maximum error in measured temperature differences was estimated to be 0.25°C. The data acquisition system was connected through an HPIB to an HP Vectra model 60 Personal Computer running HP model 3055S Data Acquisition System software.

In determining appropriate power supply settings, it was found that an imposed voltage across the heater foil of 3.5 V yielded a current draw of approximately 50 A, and that this power rate provided temperature differences which were large enough to be accurately resolvable (temperature differences typically greater than 4°C) without overheating the plate for most flow rates. The data acquisition system ran continuously during the test and took temperature scans at 15 s intervals. At the beginning of the test run the normally-impinging jet was centered over one thermocouple by moving the nozzle adjustment apparatus manually until the temperatures were radially symmetric on both sides of a single thermocouple. This established the stagnation point for the normal impingement configuration ($\alpha = 90$ deg). The ranges of flow rates available for each nozzle were limited by the water pressure available at the laboratory outlet. Additionally, at small Re the hydraulic jump approached the upstream end of the heated foil as α was decreased. In order to avoid overheating the instrumented plate, data were not taken at Re–α combinations where the hydraulic jump would cover a portion of the plate.

While the heat transfer under an obliquely impinging jet varies with both the radial and circumferential coordinates, the measurement method employed in this study (an instrumented, heated strip) permitted the acquisition of only one line of temperature data at a time. The capability to rotate the nozzle apparatus azimuthally allowed for characterization of the full two-dimensional heat transfer distribution. The principal interest of this research was to examine the effect of jet inclination on local heat transfer. Preliminary experiments revealed the effect to be most pronounced in the plane of nozzle inclination. Hence, the majority of measurements were taken with the apparatus configured to take measurements for $\phi = 0$ deg (radial heat transfer measurements coincided with the x-axis). However, measurements were also taken to characterize the azimuthal variation of the heat transfer.

The data acquisition system collected temperature measurements continuously in time, so for each configuration, the beginning and ending scan numbers were recorded along with the water flow rate and voltage and current readings. The system was allowed to reach steady state before each set of scans, so each set included only steady-state data. Temporally-averaged temperature differences, jet Reynolds numbers, local heat transfer coefficients, and local Nusselt numbers were then calculated from the heat flux, water flow, and local heated surface temperature data.

The temporally-averaged temperature difference used for the determination of heat transfer coefficients was calculated by computing the mean difference between water temperature and local plate temperature for the set of scans corresponding to each test configuration. All water properties were evaluated at the jet exit temperature. This property evaluation was appropriate near the stagnation point, where temperature differences were small, and less valid in the jet wings. However, the primary interest of this study was in the near-impingement region, $|r/d| \leqslant 3$, where the temperature differences were relatively small. Previous measurements indicated that heat losses through the back of the plate and through the bus bars were less than 0.5%, so no correction was included for such conduction losses. Additionally, an analysis of the conduction in the thin metallic foil revealed that less than 1% of the Ohmic dissipation was redistributed laterally by conjugate effects.

The maximum uncertainty in the jet Reynolds and local Nusselt numbers was determined to be 7 and 8%, respectively, using the method of Kline and McClintock [18]. This was calculated for the minimum measured temperature difference of approximately 4°C, which occurred at the point of maximum heat transfer. The uncertainty in Nusselt number at other radial locations was considerably less due to the higher measured temperature difference. As stated previously, the uncertainty in polar and azimuthal angles was estimated to be ± 1 deg. The maximum uncertainty in dimensionless radial position of the local temperature measurements was estimated to be 8 and 4% of the nozzle diameter for the small and large nozzle, respectively.

RESULTS AND DISCUSSION

Reynolds number ranges investigated in this study were 6600–40 000 for the larger nozzle ($d = 9.3$ mm) and 15 000–52 000 for the smaller nozzle ($d = 4.6$ mm). Profiles along the x-axis ($\phi = 0$ deg) were taken at jet inclination angles of $\alpha = 90$, 85, 80, 70, 60, 50, and 40 deg. In addition, measurements were made at one Reynolds number and two jet inclinations for $\phi = 0$, 15, 30, 45, 60, 75, and 90 deg for each nozzle size.

Figure 3 shows local Nusselt number profiles for the smaller nozzle as a function of inclination angle for $Re = 51\,800$, $\phi = 0$ deg. The normal jet incidence heat transfer data exhibited the trends discussed in ref. [17]. These included secondary peaks at higher Re, a region of constant local Nu for $|r/d| \leqslant 0.75$, and a dependence of local Nu on Re^a where a is a positive constant. The correlation from ref. [17] was compared to the data for normal jet incidence from this study. Although the measurements in this study were made

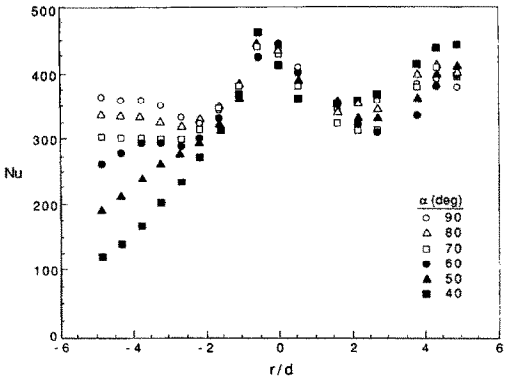

FIG. 3. Local Nusselt number profiles for various jet inclination angles, $Re = 51\,800$, $\phi = 0$ deg, $d = 4.6$ mm.

with a different heating plate assembly and different nozzle sizes than the previous study, at the stagnation point the correlation was within 12% over the full range of Re for $d = 4.6$ mm. For the larger nozzle ($d = 9.3$ mm), the correlation over predicted the measured stagnation heat transfer by a maximum of 24% at the lowest Re and by only 4% at the highest. Outside of the stagnation region, but before the transition to turbulence, the correlation described the shape of the curve quite well.

Slight asymmetry appears in the local Nusselt number data of Fig. 3, as well as data at other Reynolds numbers and nozzle size for normal impingement ($\alpha = 90$ deg). The asymmetry in these local Nusselt number data was quantified as a difference in the Nu values at corresponding radial positions on either side of the stagnation point divided by the average of the two values, $|Nu_{r/d} - Nu_{-r/d}|/0.5(Nu_{r/d} + Nu_{-r/d})$. The average asymmetry for all normal impingement data was found to be less than 5% with a maximum of only 11% out to $|r/d| = 3$ for the large nozzle and $|r/d| = 5$ for the small nozzle. This is within the estimated 8% uncertainty in local Nusselt number. This asymmetry may be explained in part by noting that the uncertainty in dimensionless radial position of any single measurement was estimated to be 4 and 8% of the nozzle diameter for the large and small nozzles, respectively.

Several general observations may be made relative to the data of Fig. 3. The point of maximum heat transfer, Nu_{max}, is seen to shift from $r/d = 0$ for normal impingement to a location upstream relative to the mean jet flow for decreasing α. A change in the magnitude of Nu_{max} is also observed, although no conclusive trend is apparent. There exists an asymmetry in the local heat transfer about the $r/d = 0$ point, and that asymmetry is accentuated for more inclined nozzles. The heat transfer for $r/d < 0$ is seen to drop, while that on the downstream side ($r/d > 0$) is seen to rise for decreasing α. A local minimum in heat transfer is observed on the downstream side at $r/d \approx 2$–3, depending on Reynolds number, after which the Nusselt number rises. This was also observed in previous work on normally-impinging nozzles [17], and is attributed to transition to turbulent flow and heat transfer. Finally, it is observed that the shape and magnitude of the Nusselt number profile is relatively insensitive to changes in nozzle inclination for $\alpha \to 90$ deg. These general observations will be explored in detail in sections to follow.

Table 1. Coefficients for equation (1) correlating local Nusselt number for $\phi = 0$ deg

d (mm)	A	a	p	m	n
4.6, $r/d > 0$	1.330	0.534	0.0968	−0.272	0.0339
4.6, $r/d < 0$	0.831	0.586	0.0696	−0.225	0.389
9.3, $r/d > 0$	4.40	0.448	0.0972	−0.243	−0.0978
9.3, $r/d < 0$	3.92	0.468	0.232	−0.658	0.788

The experimental data for the local Nusselt number profiles for $\phi = 0$ deg were correlated with an equation similar in form to that used by Goldstein and Franchett [15]

$$Nu = A\,Re^{a}\,e^{(p\alpha^2 + m\alpha + n)(r/d)} \qquad (1)$$

where α is expressed in radians. The coefficients appearing in the correlation, A, a, p, m, and n are given in Table 1. This correlation fits 99% of the data within $\pm 15\%$ and 92% of the data within $\pm 10\%$ for all measured Re, α, and for $|r/d| \leqslant 3$. The correlations do not represent the data at radial locations beyond the observed transition to turbulence noted in ref. [17], and observed in Fig. 3. As will be discussed later, the variation in heat transfer with ϕ was observed to be quite small, and was not correlated.

Another shape change visible in the local heat transfer profiles of Fig. 3 is the increasing asymmetry about $r/d = 0$ with decreasing α. Values of Nu on the downstream side ($r/d > 0$) increase while those on the upstream side drop off as α decreases. The same trend was seen for obliquely-impinging air jets [15, 16]. This behavior is not surprising in view of the positive dependence of Nu on Re for both submerged and free jets. Rubel [14] shows that the fraction of jet flow directed downstream increases rapidly with decreasing jet angle α for axisymmetric liquid jets. This causes the local Reynolds number to be much higher on the downstream side than on the upstream side, resulting in the observed asymmetry in the heat transfer profile. The asymmetry is reflected in a change in slope of the Nu–r/d profiles near the impingement point. The slope can be calculated by differentiating the Nu–r/d correlation given in equation (1) for both nozzle diameters at identical radial locations about $r/d = 0$. The slope is obviously positive on the upstream side ($r/d < 0$) and negative on the downstream side ($r/d > 0$). The correlation shows that the local Nusselt number profile becomes steeper on the upstream side (indicated by the increasing slope), and flatter on the downstream side (slope approaching zero) for decreasing α. The local heat transfer profiles are steeper on both sides for the larger nozzle.

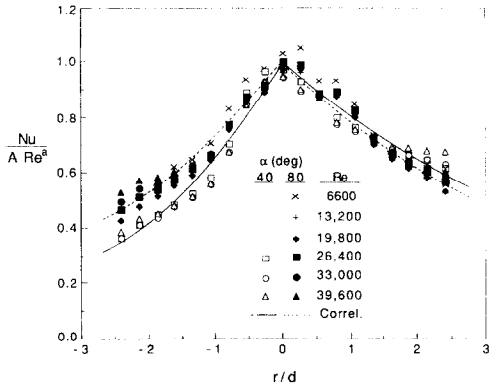

FIG. 4. Correlation of experimental local Nusselt number data for two jet inclination angles, $d = 9.3$ mm, $\phi = 0$ deg.

Figure 4 illustrates the correlation of local experimental data according to equation (1) for the large nozzle at two nozzle inclination angles, $\alpha = 80$ and 40 deg. The data for all Reynolds numbers investigated at the two jet inclination angles are shown. The local Nusselt number is normalized by the product $A\,Re^n$ given in the correlation, equation (1), in order to eliminate the dependence on Reynolds number and side (upstream or downstream) of the heat transfer profiles. The correlation represents quite well the experimental data. However, it is unable to accurately reflect the region of near-constant Nusselt number for $\alpha \to 90$ deg observed previously [17]. Consequently, the sharpness present in the experimental Nusselt number profiles near $r/d = 0$ for the more inclined ($\alpha = 40$ deg) nozzle yields better agreement with the correlation. The asymmetry in the local Nusselt number data is evident in both experimental data and correlation for both inclination angles, and is seen to be accentuated at smaller values of α.

Figure 5 compares the experimental data for the full range of jet Reynolds numbers studied and correlation for the two nozzle diameters studied at a nozzle inclination of $\alpha = 50$ deg. Again, the ratio $Nu/(A\,Re^n)$ is plotted to appropriately scale the data. Not surprisingly, the general shape of the Nu profiles is similar for the two nozzle diameters. As was observed in Fig. 4, the asymmetry in heat transfer about $r/d = 0$ is clearly evident. The figure indicates that the radial decay of the local Nusselt number in dimensionless (r/d) coordinates is smaller for the smaller nozzle.

One effect of jet inclination observed in previous work with obliquely impinging submerged jets is the shift of the point of maximum heat transfer upstream from the geometric intersection of the jet axis with the impingement plane [9–16]. This observation was also made here relative to the data of Fig. 3. In this study, the maximum shift was always less than one nozzle radius, $|s/d| \leqslant 0.5$. However, the magnitude of this shift was very close to the spatial resolution of the temperature measurements resulting from the fixed 2.5 mm spacing between the thermocouple locations ($\Delta(r/d)$ resolution: 0.27 for $d = 9.3$ mm and 0.54 for $d = 4.6$ mm). Determination of the exact location of the maximum heat transfer point was further complicated by the fact that for near-normal impingement ($\alpha \approx 90$ deg), the local Nu profile was almost flat near the impingement point, with the result that the Nusselt number at two or three locations near $r/d = 0$ were often within a few percent of one another. Due to these difficulties, the measured upstream shift of the point of maximum heat transfer was neither monotonic nor consistent. In order to deal with the restricted spatial temperature resolution and flatness of the profile in a consistent manner, five points centered around the location of maximum heat transfer were least-squares fit with a parabola for each profile. The location of the maximum in the parabola was then taken as the location of maximum heat transfer, s/d, for the corresponding Nu profile.

With s/d determined in this manner, the trend for the maximum heat transfer point to move upstream with increasing inclination angle can be clearly observed in Fig. 6. Negative values of s/d indicate an upstream shift in Nu_{max} (to negative values of r/d). Although the resolution difficulties discussed above cause too much scatter in the data for an accurate quantitative correlation, the downward slope of the least-squares line in Fig. 6 demonstrates the presence and approximate magnitude of the shift. While this

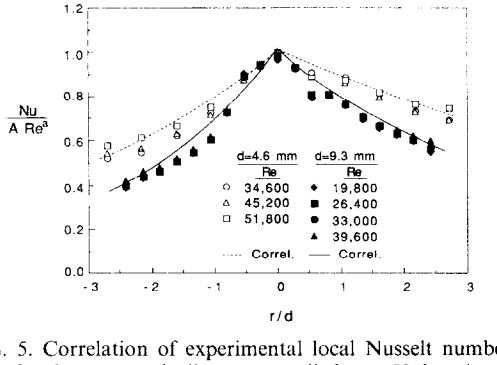

FIG. 5. Correlation of experimental local Nusselt number data for the two nozzle diameters studied, $\alpha = 50$ deg, $\phi = 0$ deg, $Pr = 9.4$.

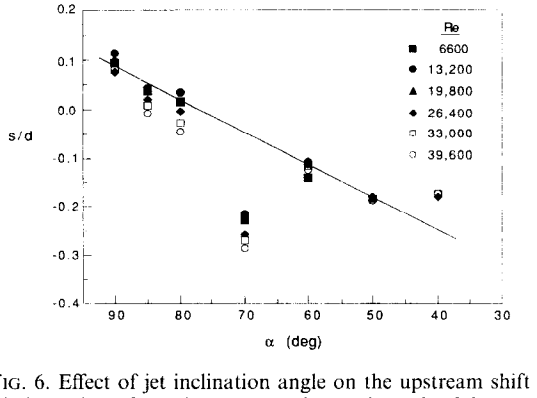

FIG. 6. Effect of jet inclination angle on the upstream shift of the point of maximum Nusselt number, $d = 9.3$ mm, $Pr = 9.4$.

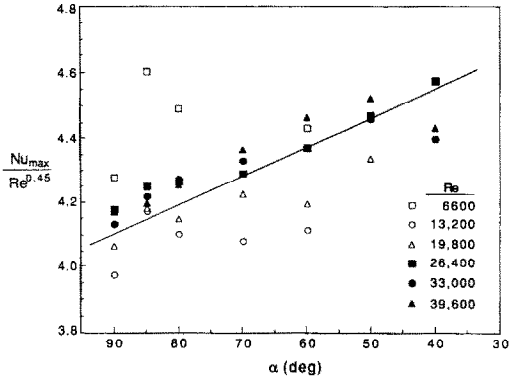

FIG. 7. Effect of jet inclination on the magnitude of the maximum Nusselt number, Nu_{max}, $d = 9.3$ mm, $Pr = 9.4$.

figure shows the magnitude of the shift determined from the maxima of the parabolas to be less than $|s/d| = 0.25$, in some cases the peak in the raw experimental profile data was seen to shift as far as $|s/d| = 0.5$. This is still significantly less than previous submerged jet measurements where normalized shifts in the maximum heat transfer of the order of 1.0–1.5 were observed for similar inclination angles [15, 16]. This can be attributed to the fact that entrainment and consequent pre-impingement spreading is a much greater factor for submerged jets than for free liquid jets. This explanation is supported by noting that in both of the aforementioned studies, the amount of shift decreased with decreasing nozzle-to-plate spacing.

Figure 7 shows the effect of inclination on the magnitude of the maximum heat transfer, Nu_{max}, for the $d = 9.3$ mm nozzle. The plot presents $Nu_{max}/Re^{0.45}$, since the correlation of equation (1) and Table 1 indicate an approximately constant dependence on $Re^{0.45}$ for the large nozzle. The Nu_{max} data were determined by scanning each experimental heat transfer profile for the maximum value. Hence, the maximum Nusselt number presented in Fig. 7 may not correspond to the s/d positions presented in Fig. 6, since the data of Fig. 6 were determined from the quadratic fit of the five highest Nusselt number data points. Despite the scatter, a generally increasing trend in Nu_{max} is observed with decreasing α, as illustrated by the least-squares linear regression of the data included in the figure. The observed increase is of the order of 10–15%. This increase in Nu_{max} for free liquid jets is at variance with the 5–30% *decrease* observed previously for inclined air jets [15, 16]. The difference between the finding of this study and the significant drop observed by Sparrow and Lovell [16] and Goldstein and Franchett [15] is again explained as an artifact of entrainment and jet spreading in the studies with submerged jets. Entrainment has the effect of decreasing the average arrival velocity, and increasing the impingement area of the jet at the plate. The increased impingement area may account for the larger dimensionless shift in the point of maximum heat transfer for the submerged jets. Further, the heat transfer coefficient in a stagnation region has been shown to be proportional to the spatial velocity gradient, dU/dr [1, 17, 19, 20]. A decrease in α (more nozzle inclination) for a submerged jet may yield a decrease in the spatial velocity gradient near the point of maximum heat transfer as jet entrainment causes interaction between the jet flow and the plate on the upstream side, and causes increasing spread in the flow on the downstream side. This decrease in the velocity gradient would cause the lower heat transfer previously observed [15, 16]. For the free liquid jet, where shear layer effects and entrainment are negligible, it may be suggested that decreasing α results in an increasingly asymmetric flow pattern, with an associated slight increase in the velocity gradient in the impingement region due to the required change in fluid flow direction of greater than 90 deg on the upstream side of the inclined jet. Hence, an increase in the Nusselt number is observed in contrast to the decrease found in submerged jets.

It was seen in Fig. 3 that the shapes of the x-axis local Nusselt number profiles change with increasing jet inclination. One aspect of these changes is that the profile comes to a sharper point in the region around the point of maximum Nu as α is decreased. The sharpness reduces the region of approximately uniform heat transfer for $|r/d| \leqslant 0.75$ for normal impingement [17]. In order to quantify this change in shape, each profile was least-squares fit with a second-order polynomial using five data points around the point of maximum Nusselt number. The leading coefficient, corresponding to one-half of the second derivative of the quadratic fit, $Nu''/2$, provides a measure of the curvature of the local Nusselt number profile. This curvature parameter is plotted as a function of jet inclination in Fig. 8 along with faired curves

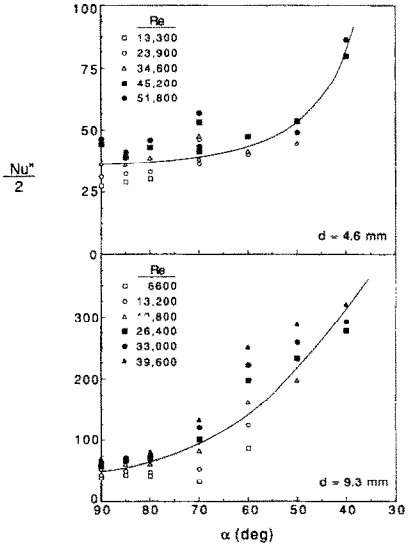

FIG. 8. Effect of jet inclination of the curvature of the local Nusselt number profiles near $r/d = 0$ for both nozzle diameters studied.

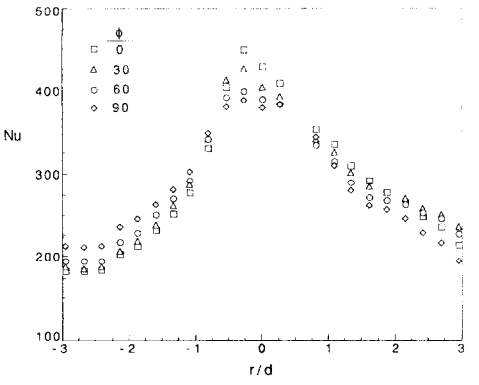

FIG. 9. Local Nusselt number profiles along diametral lines corresponding to azimuthal angles $\phi = 0$, 30, 60, and 90 deg, jet inclination angle $\alpha = 50$ deg, $Re = 26\,400$, $d = 9.3$ mm.

for $d = 4.6$ and 9.3 mm. The curvature is seen to be low near $\alpha = 90$ deg and higher for decreasing α (e.g. $\alpha = 50$ deg). The increase in curvature characteristic of more inclined jets can be clearly seen in the figure. As stated previously, the sharpening of the peak reflects the shrinking of the region of constant Nusselt number observed under normally impinging jets [17]. This increasing sharpness of the peak without a correspondingly large increase in magnitude suggests that the average heat transfer over any given region around the impingement point decreases with decreasing α. Figure 8 also illustrates that the curvature near $r/d = 0$ becomes insensitive to jet inclination at near-normal impingement, indicated by the small change in the curvature for both nozzles as $\alpha \to 90$ deg. This finding was also observed qualitatively in the local Nusselt number data of Fig. 3.

A typical azimuthal variation in heat transfer for the large diameter liquid jet is shown by Fig. 9 for a jet inclination of $\alpha = 50$ deg, $Re = 26\,400$. In order to reduce confusion in the plot, only the profiles for azimuthal angles $\phi = 0$, 30, 60, and 90 deg are shown. The data indicate a general decrease in Nu_{max} with increasing ϕ. This drop in the maximum heat transfer occurs because the line of temperature readings always passed through the geometric intersection of the jet axis and the impingement plane ($x = 0$). This point would not correspond to the point of maximum heat transfer for the inclined jet due to the upstream shift in Nu_{max} illustrated in Fig. 6. Thus, the point of maximum heat transfer would not be measured for $\phi \neq 0$ deg. Figure 9 reveals that outside of the impingement region there is only a slight change in the magnitude of the local heat transfer with azimuthal variation. For increasing ϕ, the heat transfer increases on the upstream side ($r/d < 0$) and decreases on the downstream side ($r/d > 0$). This suggests the approximate ellipsoidal regions of constant heat transfer eccentric to the impingement point illustrated for air jets in ref. [15].

Of particular interest in the presentation of the azimuthal variation data is the region of approximately constant Nusselt number near $r/d = 0$ as ϕ approaches 90 deg. This indicates that the spatially uniform heat transfer for $|r/d| \leqslant 0.75$ observed under normal impingement conditions [17] may prevail in a plane perpendicular to the axis of jet inclination ($\phi = 90$ deg in this case) even for inclined jets, $\alpha \neq 90$ deg.

The variation in local Nusselt number with varying ϕ is most pronounced in the profiles of Fig. 9 near $r/d \approx 0$. However, these differences over the full range of ϕ are generally less than 10% for $|r/d| \leqslant 3$. These results indicate that the most significant variation in the two-dimensional heat transfer distribution under an inclined impinging free liquid jet occurs in the plane of nozzle inclination (the x-axis as defined here). Accurate characterization of the dependence of local Nusselt number on inclination angle α is more critical than the influence of azimuthal variation ϕ.

CONCLUSIONS

The effect of jet inclination on the heat transfer under an obliquely impinging, round, free liquid jet striking a constant heat flux surface was examined experimentally. Measurements were taken principally along the line of intersection of the plane of nozzle inclination with the impingement surface. It was found that the point of maximum heat transfer along that line shifted upstream (with respect to the inclined jet flow) as has been observed for air jets. However, the magnitude of the shift (non-dimensionalized by the nozzle diameter) was found to be significantly less than that of the submerged jets for similar jet inclinations, and was confined to $|s/d| < 0.5$. Also differing from the submerged jet results, the magnitude of the peak heat transfer was seen to increase slightly with increasing jet inclination (lower α). Both of these differences were attributed to the relative unimportance of entrainment and pre-impingement jet spreading for the free liquid jet. The shape of the local Nusselt number profiles was significantly affected by the jet inclination. It was found that increasing inclination caused a sharpening of the peak in the Nusselt number profiles. Also with increasing inclination, the profiles exhibited an increasing asymmetry around the point of maximum heat transfer, with the upstream side of the profile dropping off much more rapidly than the downstream side. This result is to be expected in view of the positive dependence of heat transfer on Re, and the much higher local flow rates on the downstream side of the profile for oblique impingement. An empirical correlation of the experimental data along the plane of jet inclination was developed of the form $Nu = A\,Re^{a}\,e^{(px^2 + m\alpha + n)(r/d)}$ where A, a, p, m, and n are constants determined for each nozzle size and each side (upstream and downstream) of the local Nusselt number profiles.

Acknowledgements—Financial support of this work under U.S. National Science Foundation Grant CBT-8552493 is gratefully acknowledged.

REFERENCES

1. D. T. Vader, Convective and boiling heat transfer from a heated surface to an impinging planar jet of water, Ph.D. Thesis, Purdue University, West Lafayette, Indiana (1988).
2. F. F. Cadek, A fundamental investigation of jet impingement heat transfer, Ph.D. Thesis, University of Cincinnati (1968).
3. N. T. Obot, Flow and heat transfer for impinging round turbulent jets, Ph.D. Thesis, McGill University, Montreal, Quebec, Canada (1980).
4. H. Martin, Heat and mass transfer between impinging gas jets and solid surfaces. In *Advances in Heat Transfer* (Edited by J. P. Hartnett and T. F. Irvine, Jr.), Vol. 13, pp. 1–60 (1977).
5. S. J. Downs and E. H. James, Jet impingement heat transfer—a literature survey, ASME Paper 87-HT-35 (1987).
6. S. Beltaos, Oblique impingement of circular turbulent jets, *J. Hydraulic Res.* **14,** 17–36 (1976).
7. J. F. Foss, Mean flow characteristics for the oblique impingement of an axisymmetric jet, *AIAA J.* **17,** 801–802 (1979).
8. J. F. Foss and S. J. Kleis, Mean flow characteristics for the oblique impingement of an axisymmetric jet, *AIAA J.* **14,** 705–706 (1976).
9. C. D. Donaldson and R. S. Snedeker, A study of free jet impingement. Part 1. Mean properties of free and impinging jets, *J. Fluid Mech.* **45,** 281–319 (1971).
10. A. Rubel, Computations of the oblique impingement of round jets upon a plane wall, *AIAA J.* **19,** 863–871 (1981).
11. J. M. Dorrepaal, An exact solution of the Navier–Stokes equation which describes non-orthogonal stagnation point flow in two dimensions, *J. Fluid Mech.* **163,** 141–147 (1986).
12. V. K. Garg and S. Jayaraj, Boundary layer analysis for two-dimensional slot jet impingement on inclined plates, *ASME J. Heat Transfer* **110,** 577–582 (1988).
13. D. C. McMurray, P. S. Myers and O. A. Uyehara, Influence of impinging jet variables on local heat transfer coefficients along a flat surface with constant heat flux, *Proc. 3rd Int. Heat Transfer Conf.*, Vol. 2, pp. 292–299 (1966).
14. A. Rubel, Oblique impingement of a round jet on a plane surface, *AIAA J.* **20,** 1756–1758 (1982).
15. R. J. Goldstein and M. E. Franchett, Heat transfer from a flat surface to an oblique impinging jet, *ASME J. Heat Transfer* **110,** 84–90 (1988).
16. E. M. Sparrow and B. J. Lovell, Heat transfer characteristics of an obliquely impinging circular jet, *ASME J. Heat Transfer* **102,** 202–209 (1980).
17. J. Stevens and B. W. Webb, Local heat transfer coefficients under an axisymmetric single-phase liquid jet. In *Heat Transfer in Electronics 1989* (Edited by R. K. Shah), pp. 113–119. ASME, New York (1989).
18. S. J. Kline and F. A. McClintock, Describing uncertainties in single-sample experiments, *Mech. Engng* 3–12 (January 1953).
19. D. A. Zumbrunnen, F. P. Incropera and R. Viskanta, Convective heat transfer distributions on a plate cooled by planar water jets, *ASME J. Heat Transfer* **111,** 889–896 (1989).
20. L. C. Burmeister, *Convective Heat Transfer*. Wiley, New York (1972).

EFFET DE L'INCLINAISON SUR LE TRANSFERT THERMIQUE LOCAL POUR UN JET LIQUIDE LIBRE AXISYMETRIQUE

Résumé—On étudie expérimentalement l'effet de l'inclinaison sur le transfert thermique local pour un jet liquide rond qui attaque obliquement une surface chauffée à flux constant. Les paramètres du problème sont le nombre de Reynolds entre 6600 et 52 000, l'inclinaison du jet entre 40 et 90 degrés à partir de l'horizontale. Les expériences sont conduites pour deux diamètres de tuyère $d = 4{,}6$ et 9,3 mm. On trouve que le point de transfert maximal le long des x (ligne d'intersection du plan d'inclinaison du jet avec la surface) est déplacé en amont et varie en fonction de l'inclinaison du jet, avec un maximum de 0,5 fois le diamètre de l'orifice. On trouve aussi que la forme des profils de nombre de Nusselt le long des x change quand le jet est incliné. Un de ces changements est la raideur du pic au point du transfert thermique maximal. Un autre changement est l'accroissement de la disymétrie autour du point de transfert maximal avec la branche en amont du profil descendant plus rapidement que la brancho on aval. Quelques mesures sont faites pour caractériser la distribution bidimensionnelle du transfert thermique pour le jet incliné. Des formules sont développées pour la variation radiale du transfert thermique local dans le plan d'inclinaison du jet.

EINFLUSS DES NEIGUNGSWINKELS AUF DEN ÖRTLICHEN WÄRMEÜBERGANG UNTER EINEM ACHSENSYMMETRISCHEN FREIEN FLÜSSIGKEITSSTRAHL

Zusammenfassung—In der vorliegenden experimentellen Arbeit wird die Abhängigkeit des örtlichen Wärmeübergangs von dem Winkel untersucht, unter dem ein kreisrunder freier Flüssigkeitsstrahl auf eine Oberfläche mit konstanter Wärmestromdichte auftrifft. Der Einfluß folgender Parameter wird untersucht: Reynolds-Zahl des Strahls (6600 bis 52 000), Neigungswinkel des Strahls (40 bis 90 Grad gegenüber der Waagerechten), Düsendurchmesser ($d = 4{,}6$ und 9,3 mm). Es zeigt sich, daß die x-Achse (dies ist die Schnittlinie der Neigungsebene des Strahls und der festen Oberfläche) einen Punkt mit maximalem Wärmeübergang aufweist, welcher abhängig vom Neigungswinkel um maximal einen halben Düsendurchmesser stromaufwärts verschoben ist. Außerdem ist zu beobachten, daß sich die Form des Profils der örtlichen Nusselt-Zahl entlang der x-Achse mit dem Neigungswinkel verändert. Eine dieser Veränderungen ist eine Verschärfung der Spitze im Profil am Ort des maximalen Wärmeübergangs. Eine weitere Veränderung äußert sich in einer zunehmenden Asymmetrie in der Umgebung des Punktes maximalen Wärmeübergangs, wobei sich stromaufwärts ein steilerer Abfall zeigt als stromabwärts. Die vollständige zweidimensionale Verteilung des Wärmeübergangs unter dem geneigten Strahl wird mit Hilfe einiger Messungen gezeigt. Es werden Korrelationen zur Beschreibung der radialen Verteilung des örtlichen Wärmeübergangs in der Neigungsebene der Düse entwickelt.

ВЛИЯНИЕ УГЛА НАТЕКАНИЯ СТРУИ НА ЛОКАЛЬНЫЙ ТЕПЛОПЕРЕНОС ОТ ОСЕСИММЕТРИЧНОЙ СВОБОДНОЙ СТРУИ ЖИДКОСТИ

Аннотация—Экспериментально исследуется влияние угла натекания струи на локальный теплоперенос в случае круглой свободной струи жидкости, ударяющейся о поверхность с постоянным тепловым потоком. Исследуется влияние числа Рейнольдса в интервале 6600–52 000 и угла натекания, изменяющегося от 40 до 90°. Эксперименты проводятся для двух диаметров сопла: $d = 4{,}6$ и 9,3 мм. Найдено, что точка максимального теплопереноса по оси x (линия пересечения плоскости угла натекания струи с поверхностью) смещается вверх по потоку (относительно струйного течения) в зависимости от наклона струи максимум на 0,5 диаметров сопла. Кроме того, обнаружено, что форма профилей числа Нуссельта по оси x изменяется с накломон струи. Одно из этих изменений заключается в заострении пика профиля у точки максимального теплопереноса, другое—в увеличении асимметрии относительно точки максимального теплопереноса, когда сторона профиля вверх по потоку снижается быстрей стороны вниз по потоку. Некоторые измерения используются для характеристики полного двумерного распределения теплопереноса от наклонной струи. Выводятся обобщенные соотношения для радиального изменения локального теплопереноса в плоскости наклона сопла.